



Shaking Table Test of Liquefiable Site-Bucket Foundation-Offshore Wind Turbine Structure Seismic Response

Haibin Xu¹, Kaiyuan Liu^{1,*}, Xiaogang Jia², Shiping Lan²
Weiyu Ling³, Chaoyue Li³, You Xie³

¹China Three Gorges Corporation, Beijing, 101100, China

²China Three Gorges Corporation Fujian Branch, Fuzhou, 350012, China

³Key Laboratory of Urban Security and Disaster Engineering of Ministry of Education, Beijing University of Technology, Beijing, 100124, China

*Liuky@163.com.cn

Abstract. In order to explore the dynamic response of the superstructure and the deformation characteristics of the site after sand liquefaction of offshore wind turbine foundation under the combined action of wind, wave and earthquake, a large-scale shaking table test of offshore wind turbine suction bucket considering the combined load of wind and wave. According to the research objective and purpose, this paper expounds the overall design scheme of the test, the design and preparation of the site and structure, the selection and layout of the sensor, and the selection and working conditions of the wind, wave and seismic load. The test results show that under the action of 0.35 g EL Centro wave, the saturated sand site is completely liquefied, the site loses its bearing capacity, the single bucket foundation is inclined and pulled out, and the bucket foundation is completely invalid. In this paper, the variation law of pore pressure and acceleration after liquefaction of saturated sand site is analyzed. This experiment has achieved the expected goal, indicating that the series of experimental design is reasonable.

Keywords: Suction bucket foundation; Experimental design; Shaking table test; Wind-wave combined load; Seismic response.

1 Introduction

In recent years, offshore wind turbine has developed rapidly. By the end of 2022, the global cumulative installed capacity of offshore wind power reaches 64.3GW, of which China ranks first with 31.44GW cumulative installed capacity of offshore wind power. China has abundant offshore wind energy resources, which is three times that of on-shore wind energy resources[1]. China's offshore wind power development has broad prospects

Compared with the traditional pile foundation, the suction bucket foundation has a simpler design, more economical construction cost, can be applied to deeper sea area, expanding the buildable area of offshore wind power. Offshore wind power foundation

© The Author(s) 2024

F. Ding et al. (eds.), *Proceedings of the 2024 International Conference on Civil Engineering Structures and Concrete Materials (CESCM 2024)*, Advances in Engineering Research 247,

https://doi.org/10.2991/978-94-6463-564-5_12

should not only consider the impact of sea wind, waves on the wind power structure, but also consider the impact of earthquakes on the wind power structure when it is in the earthquake-frequent area. Therefore, the working performance and dynamic response of offshore wind turbine single-bucket foundation under the combined action of various loads have attracted the attention of the academic community. Zhu Fangyuan et al. [2] found the effect of the change of cyclic loading direction on the foundation stiffness and ultimate bearing capacity of suction bucket; Yuan Minghui et al. [3] investigated the bearing characteristics of the clay site-suction bucket foundation system under the combined effect of wind and wave loads; Li Yameng et al. [4] analyzed the damage mechanism of horizontal and vertical loads on suction bucket foundations in clay through indoor simulation tests; Xie Yinbiao et al. [5] investigated the damage mechanism of suction bucket foundations in clay by indoor simulation tests to study the effects of wind and wave cyclic loads on the bearing capacity of suction bucket. The results show that under cyclic loading, the horizontal bearing capacity of the foundation increases with the increase of foundation burial depth; The larger the cyclic load, the lower the bearing capacity of the foundation; Li Jingyi et al. [6] carried out a large-scale shaking table test to analyze the superporous water pressure and acceleration of single and composite bucket foundations under seismic action, and clarified the inhibition effect of the bucket foundation on superporous water pressure and acceleration. Luo Lunbo et al. [7] investigated the relationship between cyclic loading and horizontal bearing capacity of suction bucket foundation through indoor model test; Liu Xixi [8] investigated the effects of wave height, suction bucket dimensions and peripheral scour of suction bucket foundation; Nielsen et al. [9] investigated the effects of suction bucket foundation under cyclic loading in saturated dense sand on the suprapore hydraulic pressure and cumulative turning angle of foundation soil; Liu Meimei et al. [10] investigated the effect of different height-to-diameter ratios of suction bucket on bearing capacity and illustrated the damage mechanism of suction bucket under horizontal loading; Kou Hailei et al. [11] investigated the effect of different load cycling ratios on the bearing capacity and cumulative corner of suction bucket in sandy foundation through indoor simulation tests.

At present, domestic and foreign scholars have done a lot of research on the bucket foundation of offshore wind turbines, but there is still a lack of research on its seismic performance. Due to the large stiffness of the structure itself, the probability of structural damage under the action of earthquake is small. The important reason for the failure of the foundation is that the liquefaction of the foundation soil leads to the excessive displacement of the foundation structure, and then loses the bearing capacity. In this paper, the dynamic response law of offshore wind turbine single bucket foundation in liquefiable site under the combined action of horizontal load and earthquake is carried out by 1g shaking table test, and the factors of bucket foundation instability are analyzed.

2 Description of Large-Scale Shake Table Test

2.1 Test Facilities

The overall objective of this test is to study the dynamic response of single-cylinder offshore wind turbine under seismic load, to reveal the dynamic response of offshore wind turbine superstructure and the deformation characteristics of the site under the combined action of wind and wave load. The wind turbine model is based on a 6.45 MW wind turbine. The test is divided into two stages: (1) The cyclic action stage of wind wave load on wind turbine structure. (2) The combined action of wind wave load and earthquake.

The test was carried out on the simulated earthquake shaking table in the Seismic Testing Laboratory of Beijing Institute of Technology. The main technical parameters are as follows: the table size is 3 m×3 m, the working frequency is 0.4-50 Hz, the maximum load is 10 t, the maximum tilting moment is 30 t-m, the maximum acceleration that can be exerted in the horizontal direction when the table is fully loaded is 1.0 g, and the maximum velocity is 600 mm/s. As shown in Fig. 1, the net dimensions of the laminar shear model soil box were: length 2.5 m, width 1.4 m, height 1.38 m.



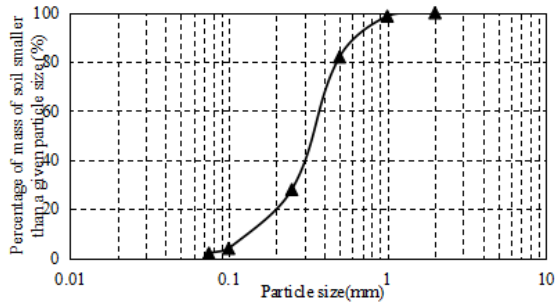
Fig. 1. Laminar shear box and shaker table top view

2.2 Site Properties and Preparation

In order to simulate the use of actual single-cylinder offshore wind power foundation, the test site is composed of 0.02 m clay layer, 0.48 m saturated sandy soil layer with 60% uniformity and 0.7 m dense sand layer with 85% densification from top to bottom. A river sand was used for the test, and the physical properties of the adopted sand and soil were tested before the test, and the parameters of the sand used for the test were obtained as shown in Table 1, and the particle grading of the sand and soil was shown in Fig. 2.

Table 1. Physical parameters of saturated sand

Maximum dry density/(g/cm ³)	Minimum dry density/(g/cm ³)	Unevenness coefficient	Maximum Pore Ratio	Minimum Pore Ratio	Relative Density / (%)
1.64	1.33	2.86	0.985	0.608	60

**Fig. 2.** Sand particle grading curve for testing

The dense sand layer at the bottom layer is prepared by the combination of layered compaction and static pressure., the saturated sand layer is prepared by sand rain method. [12]. The water table line was set on the surface of the saturated sand soil layer. At the same time, 0.02m thick clay layer was prepared above the saturated sand soil layer. After the site preparation was perfected, it was rested for 12h to ensure that the sandy soil layer was fully saturated and then the test was carried out.

2.3 Bucket Foundation-superstructure Design and Fabrication

The main focus of this test is to qualitatively analyze the effect of environmental loads such as wind and waves on the seismic response of the cylinder foundation from a research point of view, thus focusing on the similarity ratio between the site and structural stiffness. The ground structure takes inertia force and lateral stiffness as control factors. According to Buckingham- π theorem, the model structure selects length, elastic modulus and acceleration as the basic physical quantities; the model soil selects shear wave velocity, density and acceleration as the basic physical quantities, and the similarity relationship of the model system can be determined, which is shown in Table 2.

Table 2. Model system similarity relationships and similarity ratios

Typology	Physical quantity	Resemblance	Similarity ratio	
			Modelling	Modelled foundation soil
Geometric feature	Length S_l	S_l	1/70	1/4
	Linear displacement r	$S_r = S_l$	1/70	1/4
Material	equivalent density ρ	$S_\rho = S_E / S_l S_a$	70	1

characteristics	modulus of elasticity E	S_E	1	/
	Soil shear wave speed V_s	S_v	/	1/2
	Shear modulus of soil G	S_G	/	1/4
	bending rigidity EI	$S_{EI} = S_E S_I^4$	$1/70^4$	/
	compressive stiffness EA	$S_{EA} = S_E S_I^2$	$1/70^2$	/
Dynamic behaviour	Mass m	$S_m = S_\rho S_l^3$	$1/(4*70^2)$	/
	Force F	$S_F = S_\rho S_l^3 S_a$	$1/(4*70^2)$	/
	Stresses σ	$S_\sigma = S_l S_a S_\rho$	1/4	1/4
	Strains ϵ	$S_\epsilon = S_l S_a S_\rho / S_E$	1	1

The superstructure of the wind turbine is simplified into mass blocks. The prototype of the single-cylinder-base-superstructure and the dimensions of the model after 1:70 similarity ratio similarity are shown in Table 3. The model of the cylinder foundation-superstructure is shown in Fig. 3.

Table 3. Bucket foundation-superstructure prototype and model dimensions

Physical quantity	Original form	Model
Tower length/m	85	1.2
Tower wall thickness/mm	60	1
Tower diameter/m	7.5	0.1
Transition section wall thickness /mm	75	1
Diameter of transition section /m	10	0.14
Bucket wall thickness/mm	60	1

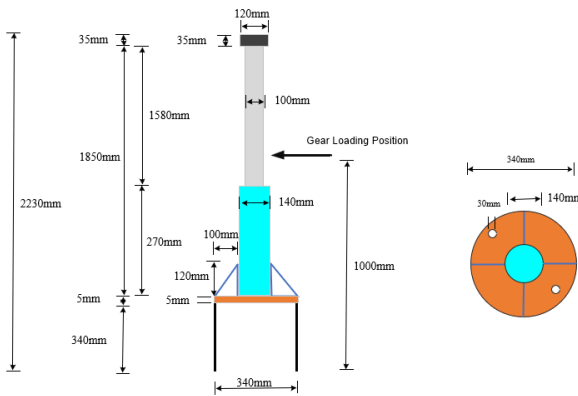


Fig. 3. Schematic diagram of monocular foundation and superstructure

2.4 Sensor Selection and Layout

In order to study the seismic response law of single bucket foundation, accelerometers and pore pressure gauges are arranged at different depths in the bucket foundation. Accelerometers and pore pressure gauges are arranged near the outer wall of the cylinder at the same depth to study the seismic response. The accelerometer and pore pressure

meter are arranged far away from the cylinder wall to study the seismic response law of the free field site. Strain gauges are symmetrically arranged along the seismic direction on the cylinder wall and the tower structure to measure the strain response of the structure. Accelerometers are arranged at the top of the structure and in the middle of the tower to measure the dynamic response of the structure. The sensor layout of monocular foundation test is shown in Fig. 4.

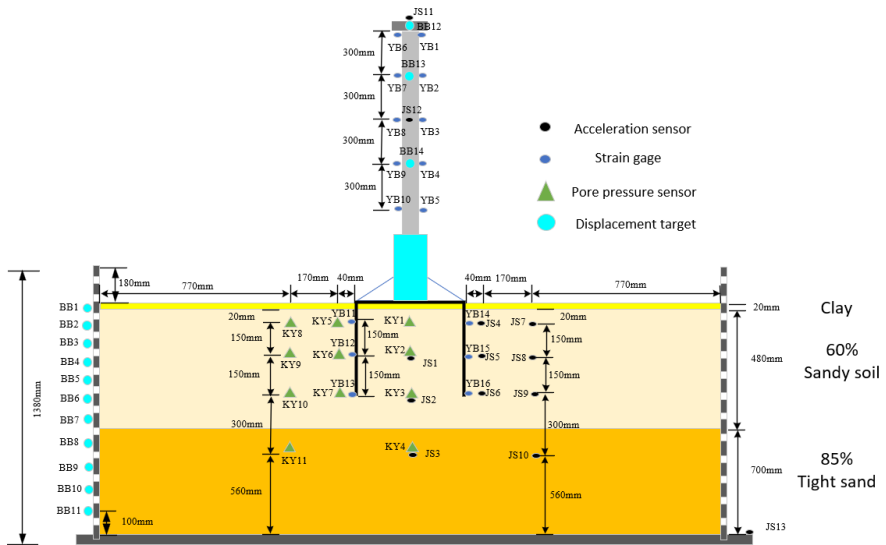


Fig. 4. Schematic diagram of single-barrel sensor layout

2.5 Ground Vibration Selection and Input Program

In this experiment, white noise, LEAP wave and EL-Centro wave were selected as the input shock. The seismic acceleration time scale and Fourier spectrum are shown in Fig. 5 and Fig. 6. In order to study the seismic response of the system when the soil is not sufficiently softened under small earthquake excitation, the small earthquake excitation process of leap wave with a peak value of 0.1g and the liquefaction process of EL-Centro wave with a peak value of 0.35g are input. Table 4 shows the test loading scheme. In order to ensure that the excess pore water pressure of the site can be completely dissipated, sufficient time left between two seismic loads.

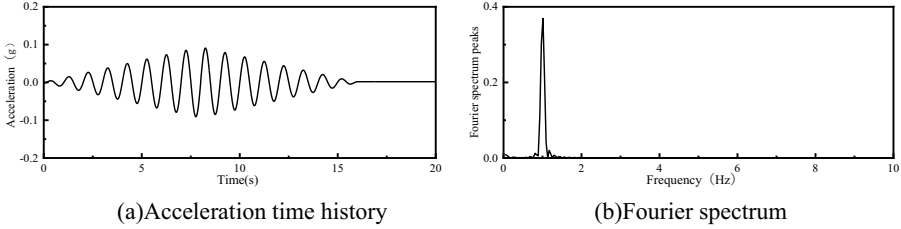


Fig. 5. Time history and Fourier spectrum of LEAP earthquake acceleration

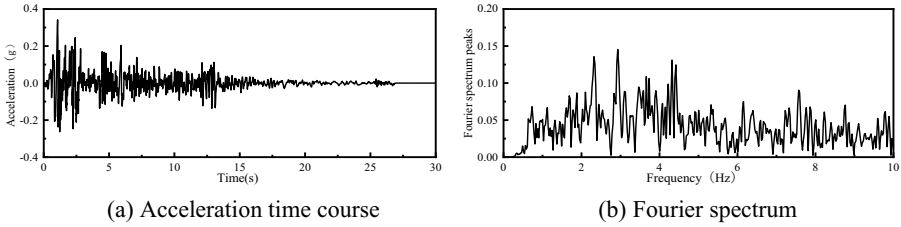


Fig. 6. EL-Centro seismic acceleration time course, Fourier spectrum

Table 4. Test loading conditions

Motion	Ground motion ID	Peak ground acceleration /g	Time/s	Interval time between events /min
1	White noise	0.1	30	-
2	Leap	0.1	30	30
3	White noise	0.1	30	-
4	El-Centro	0.35	30	30
5	White noise	0.1	30	-

2.6 Selection and Application of Combined Wind and Wave Loads

With a hub height of 110m and an impeller diameter of 175m, the wind load acting on the blades of the 6.45MW model can be up to 2MN, while the horizontal load caused by wave action can be approximated as a sinusoidal load with a size of 4MN at 40m above the mud surface. Therefore, the loads on the 6.45 MW model are as follows:

$$\text{Horizontal load } F = F_f + F_t = 6MN .$$

$$\text{Overturning moment } M = F_f \times L_f + F_t \times L_t = 460MN \cdot m .$$

The horizontal combined force is 6MN and the overturning moment is 460MN-m, which is equivalent to the sinusoidal load applied at a position about 80m above the mud surface. According to the similarity ratio of 1:70, the test load is a horizontal sinusoidal load of 20N applied at a position 1m from the bottom of the cylinder foundation, and the sinusoidal load is applied by a high-precision servo motor gear unit.

3 Preliminary Results of the Experiment

3.1 Pore Pressure Ratio of Saturated Sand Layer and Dense Sand Layer

Fig. 7 shows the time history of excess pore pressure ratio of dense sand layer and saturated sand layer under 0.35 g ground motion test condition, where KY8 is the top measuring point of saturated sand layer, KY10 is the bottom measuring point of saturated sand layer, and KY11 is the measuring point of dense sand layer. From the diagram, it can be seen that when the 0.35 g EL-Centro ground motion input, the excess pore pressure ratio of the saturated sand layer all reaches 1, the saturated sand layer is completely liquefied, the excess pore pressure ratio of the dense sand layer is 0.5, and the dense sand layer is not liquefied.

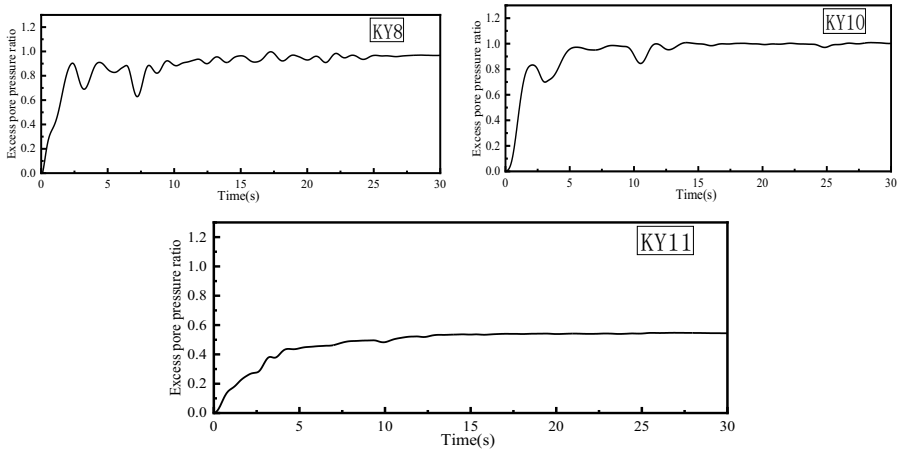


Fig. 7. Partial time history of soil excess pore pressure ratio

3.2 Soil Acceleration Response

Fig. 8 shows the acceleration time history of soil under the ground motion test condition of 0.35g. It can be seen from the figure that the dense sand layer has an amplified effect on the soil acceleration, while the saturated sand layer significantly decreases the soil acceleration. This is because the saturated sand layer of the site is liquefied under the action of strong earthquake, the soil stiffness decreases, the shear wave is difficult to transmit upward, and the acceleration decreases rapidly. At the same time, it can be seen that the combined load of wind and wave has little influence on the site. Fig. 9 shows the Fourier spectrum of soil acceleration under ground motion test conditions of 0.35g. Compared with the Fourier spectrum of the original wave in Fig. 7, it can be seen that the liquefaction of the site will cause the high-frequency part to be filtered and the low-frequency part to be amplified.

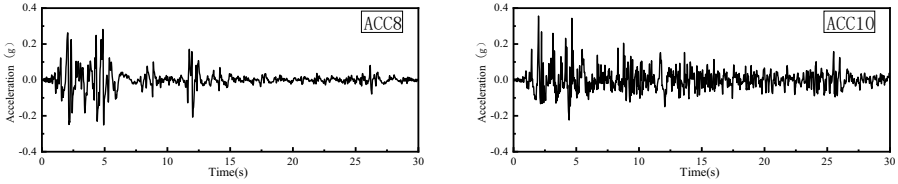


Fig. 8. Time history of soil acceleration

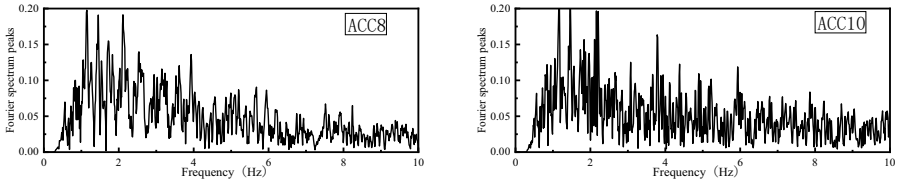


Fig. 9. Fourier spectrum of soil acceleration

3.3 Seismic Response Macro Phenomena and Failure Modes

As shown in Fig. 10, comparing the surface state of the soil before and after the test, it can be found that there is less water on the surface of the soil before the test, and the surface is flat. After the input of 0.35 g EL seismic record, there is a large amount of water on the surface of the soil layer, and there are multiple sandblasting water points on the surface of the soil, accompanied by sand gushing. This phenomenon also shows that the saturated sand layer has been completely liquefied.



(a) Water bubbling up from sandblasting on the soil surface

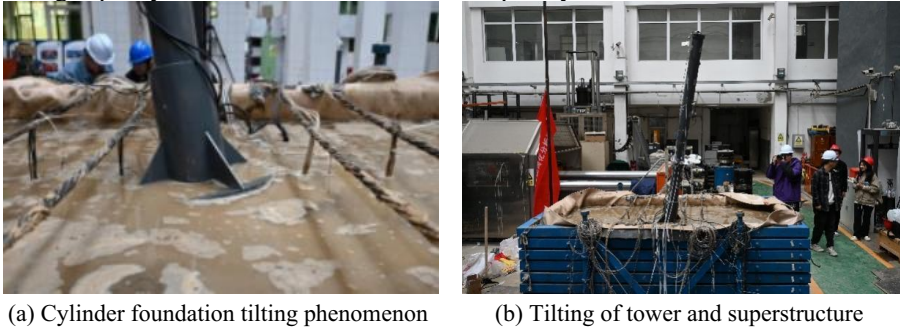


(b) Water accumulation on the soil surface after the test

Fig. 10. Soil surface before and after the test

As shown in Fig.11, Under the action of 0.35 g EL wave earthquake, the bucket foundation and the upper structure are significantly inclined. The settlement on the side of the bucket foundation reaches 5 cm, the horizontal displacement of the tower top along the seismic direction reaches 30 cm, and the inclination angle of the tower top reaches 10 °, which exceeds the design requirements of the specification. There is a significant pull-out phenomenon at the bottom of the bucket foundation, which is

consistent with the failure mode of the bucket foundation predicted in the experimental design. This also shows that the fully liquefied saturated sand layer completely loses its bearing capacity and the bucket foundation completely fails.



(a) Cylinder foundation tilting phenomenon

(b) Tilting of tower and superstructure

Fig. 11. Inclination of test cylinder foundation and superstructure

4 Conclusion

This paper introduces in detail the scheme and design method of single-bucket foundation vibration table test for offshore wind turbine considering the combined action of wind, wave and seismic loads. The liquefaction law of the site under earthquake is briefly analyzed. The main conclusions are as follows:

(1) According to the results of the experiment of saturated sand ground liquefaction phenomenon, significantly more than phenomenon, water spray take sand liquefaction of super pore pressure ratio reflects the saturated sand layer all reach liquefaction, acceleration and liquefied layer are obviously inhibited effect.

(2) The results after recreates the saturated sand liquefaction monocular tilted foundation after loss of bearing capacity of structure formation and the barrel of foundation settlement, pull out the macroscopic phenomenon along the direction of earthquake ground motion input, achieve their goals and record the reliable data.

There are still some deficiencies in this study:

(1) In this study, the bucket foundation is completely in the saturated sand site, while in the actual project, the bucket foundation may be partially in the saturated sand foundation. Therefore, further analysis of various soil conditions can be carried out in the next study.

(2) Due to the limitation of test equipment conditions, the wind and wave loads considered in this study are only simplified to concentrated simple harmonic waves acting on the tower barrel. In the follow-up study, the influence of wind and wave loads on the wind turbine can be further considered.

Acknowledgement

Supported by the China Three Gorges Corporation research project NBZZ202200447 and NBZZ202300604.

References

1. Yan XR, Zhang NN, Ma KC, et al. (2024) Overview of the current situation and trend of offshore wind power development in China. *Power Generation Technology*, 45(01):1- 12. DOI: 10.12096/j.2096-4528.pgt.23093.
2. Zhu FY, Birtta B, et al. (2018) The response of suction caissons to multidirectional lateral cyclic loading in sand over clay. *Ocean Engineering*, 17043-54.
3. Yuan MH. (2023) Bearing characteristics of suction bucket foundation in saturated soft clay under cyclic wind and wave loading. Qingdao University of Technology, DOI: 10.27263/d.cnki.gqudc.2023.000705.
4. Li YM, Wu K, Luo HT. (2021) Experimental study on destabilization damage mode of marine suction caisson foundation. *Engineering Technology Research*, 6(07):56-57. DOI: 10.19537/j.cnki.2096-2789.2021.07.022.
5. Xie YB, Luo HT, Li YM, et al. (2022) Bearing capacity characteristics of suction type barrel foundation under cyclic loading in sandy soil. *Journal of Shandong University (Engineering Edition)*, 52(04):151- 156.
6. Li JY. (2020) Comparative study on liquefaction resistance of sandy soil foundation with single-cylinder foundation and composite-cylinder foundation for offshore wind power. Tianjin University. DOI:10.27356/d.cnki.gtjdu.2020.001713.
7. Luo LB, Wang Y, Huang JQ ,et al. (2021) Study on the effect of oceanic cyclic loading on the horizontal bearing capacity of suction drum foundation. *Journal of Solar Energy*, 42(03):142- 147. DOI:10.19912/j.0254-0096.tynxb.2020-0011.
8. Liu XX, Chen XG, Feng T, et al. (2019) Experimental study on scour characteristics of barrel-shaped foundation under wave action. *Ocean Engineering*, 37(06):104- 113+121. DOI:10.16483/j.issn.1005-9865.2019.06.011.
9. Nielsen D.S, Ibsen B.L, Nielsen N.B. (2017) Response of Cyclic-Loaded Bucket Foundations in Saturated Dense Sand. *Geoenvironmental Engineering*, 143(11).
10. Liu MM, Lian JJ, Yang M. (2017) Experimental and numerical studies on lateral bearing capacity of bucket foundation in saturated sand. *Ocean Engineering*. 144(14).
11. Kou HL, Zhou N, Yang DL, et al. (2021) Experimental study on horizontal bearing characteristics of suction drum foundation for offshore wind turbine in sandy soil foundation. *Journal of Engineering Geology*, 29(06):1752- 1758. DOI:10.13544/j.cnki.jeg.2021-0202.
12. Jia KM, Xu CS, Du XL, et al. (2023) Design of large-scale shaking table test program for seismic damage response of liquefied lateral extension site-group pile foundation-structure system. *Engineering Mechanics*, 40(07):121- 136.

Open Access This chapter is licensed under the terms of the Creative Commons Attribution-NonCommercial 4.0 International License (<http://creativecommons.org/licenses/by-nc/4.0/>), which permits any noncommercial use, sharing, adaptation, distribution and reproduction in any medium or format, as long as you give appropriate credit to the original author(s) and the source, provide a link to the Creative Commons license and indicate if changes were made.

The images or other third party material in this chapter are included in the chapter's Creative Commons license, unless indicated otherwise in a credit line to the material. If material is not included in the chapter's Creative Commons license and your intended use is not permitted by statutory regulation or exceeds the permitted use, you will need to obtain permission directly from the copyright holder.

